JOURNAL OF SOLID STATE CHEMISTRY 114, 1–5 (1995)

Homogeneity Range and Some Physical Properties of Intercalation Compounds of Mn_xTaS_2

Hirofumi Hinode, Tsukio Ohtani,* and Masataka Wakihara[1]

Department of Chemical Engineering, Tokyo Institute of Technology, 2-12-1, Ookayama, Meguro-ku, Tokyo 152, Japan; and
**Department of Chemistry, Okayama University of Science, 1-1, Ridai-cho, Okayama 700, Japan*

Received August 9, 1993; accepted March 3, 1994

The intercalation compounds of Mn_xTaS_2 were synthesized by heating a mixture of TaS_2 and Mn metal in an evacuated silica tube. The single-phase region was determined to be $0.20 \leq x \leq 0.50$ in Mn_xTaS_2 at 1000°C. The hexagonal *c*-axis increased simply with increasing manganese content *x*, while the *a*-axis had anomalies at $x = 1/4$ and 1/3 where different superlattices were observed. The temperature dependence of electrical resistivity showed metallic behavior. The temperature variation of magnetic susceptibility obeyed a Curie–Weiss law. The Weiss constant (paramagnetic Curie temperature) θ decreased with *x* and the value changed from positive to negative at $x = 0.50$, suggesting the change of exchange interactions from ferromagnetic to antiferromagnetic. The valance state of manganese in Mn_xTaS_2 was evaluated as divalent by P_{eff} (effective Bohr magneton) calculated from the Curie constant.

INTRODUCTION

One of the most striking features in the quasi-two-dimensional transition metal dichalcogenides MX_2 is the charge density wave (1). Another interesting property is an intercalation effect. Most of the atoms and many of the organic molecules of the Lewis base can be intercalated in the van der Waals gap sites between two neighboring sulfur layers. A drastic property change in the intercalation compounds can be found in transport phenomena; for example, the intercalation of alkali atoms in semiconductive MoS_2 or $ZrSe_2$ converts the mother crystals into metals, and the intercalation compounds show superconductivity at low temperatures (2, 3).

MX_2 (M = Mo, Nb, and Ta; X = S and Se) with the $2H$ polytype structure forms intercalation compounds with the first-row transition elements as T_xMX_2. The transition metals, such as V, Cr, Mn, and Fe, occupy octahedral sites between the trigonal prismatic mother crystal layers. T_xMX_2 is particularly interesting because the transition metals form ordered $2a_0 \times 2a_0$ and $\sqrt{3}a_0 \times \sqrt{3}a_0$ superstructures for $x = 1/4$ and 1/3 in T_xMX_2, respectively, where a_0 is the lattice parameter of the hexagonal basal plane of the host MX_2 crystal (4, 5). Also, the transition metals, such as copper, occupy tetrahedral holes between the prismatic sulfur layers (6).

The host compound, TaS_2, consists of *d*-band metal, with one electron in the Ta-derived *d* band. For the trigonal prismatic coordination of the Ta ($2H$ polytype), the lowest lying states belong to a subband of width ≈1 eV, split off from the rest of the *d* bands by a hybridization gap of ≈1 eV, and of d_{z^2}, d_{xy}, and $d_{x^2-y^2}$ character (7). This subband is half filled for the group V materials, such as Ta. In these intercalation complexes, there is ample evidence for charge transfer from the $3d$ transition metal to the Ta *d* band, resulting in oxidation states of +2 or +3 for the transition metal ion. The increased filling of the *d* subband that results was observed most clearly in the photoemission experiments of Clark (8). The rigid-band approximation, in which the nature of the Ta *d* band is considered to be unaffected except in the degree of band filling, is in good agreement with experimental results (9, 10).

Most of the previous magnetic susceptibility studies on these intercalates were made on powders above the temperature of liquid nitrogen. In general, there is poor agreement between different workers regarding the values of magnetic parameters of complexes with the same nominal composition because of impurities, varying intercalate concentrations, and, in some cases, a limited temperature range over which the data are fitted. This has led to some controversy concerning the valance states of the different intercalate ions. The valence state of the transition metal in T_xMX_2 was determined from the magnetic moment estimated from the Curie–Weiss law. This estimate is applicable in insulators, but there are problems in applying it to metals because the *d* orbitals often are delocalized. Nevertheless, single-crystal measurements, including optical, transport, and magnetic measurements for carefully characterized materials, show clearly that the V and Cr intercalate ions are trivalent, whereas the Mn, Fe, Co,

[1] To whom correspondence should be addressed.

0022-4596/95 $6.00

and Ni ions are divalent for both $x = 1/4$ and $1/3$ in T_xMX_2 (7, 9–11).

For the Mn_xTaS_2 compounds, the occurrence of superstructures has been reported only for manganese contents x equal to 1/4 and 1/3 (12–14). In the present study, we have synthesized Mn_xTaS_2 compounds with various manganese contents and have determined the single phase region of Mn_xTaS_2 using powder X-ray diffraction. The physical properties of samples in the single phase region, such as electrical resistivity, magnetic susceptibility, and the ESR spectrum, have then been studied.

EXPERIMENTAL

Synthesized TaS_2 (from Ta foil and elemental sulfur) and Mn metal powder (Soekawa Chemical Co., 99.9%) were used as the starting materials for the preparation of the intercalation compounds Mn_xTaS_2. The detailed synthetic procedure was described elsewhere (15).

We first used Mn powder as purchased, but the synthesized sample included some oxide (Ta_2O_5). We thought the surface of the Mn powder was covered with a thin oxide layer, so we used Mn metal after heating it under vacuum at 300°C for 12 hr. The mixture of the TaS_2 and the Mn metal powder in the desired ratio was ground in an agate mortar and pressed into a pellet. The pellet was sealed in an evacuated silica tube and annealed first at 400°C for 12 hr and then at 1000°C for 7 days, followed by quenching in ice water. The sample was ground, sealed again, heated at 1000°C for 7 days, and again quenched. All the samples were identified by powder X-ray diffractometry (Rigaku X-ray diffractometer Rotaflex RU-200A, Cu$K\alpha$ radiation).

The electrical resistivity measurement on the pellet sample (4 mm diameter × 8 mm thickness) was performed using the standard dc four-probe technique under H_2 atmosphere in the temperature range 90–300 K. However, the measurement for $Mn_{0.25}TaS_2$ could not be carried out because of the difficulty of sintering.

The magnetic susceptibilities were measured using the Faraday method in the temperature range 80–300 K. Electron spin resonance (ESR) was recorded on a conventional X-band spectrometer (JEOL JES RE-1X) at room temperature to identify the presence of Mn^{2+}. The electron diffraction patterns was taken by using 200 kV electron microscopy (JEOL 200FX).

RESULTS AND DISCUSSION

Figure 1 shows the schematic figures of three polytype structures for M_xTaS_2. In the case of Mn, Fe, and Cr, the M atoms occupy the octahedral holes in the van der Waals gap between the layers of the host TaS_2. The TaS_2 layers have trigonal prismatic symmetry and adopt the

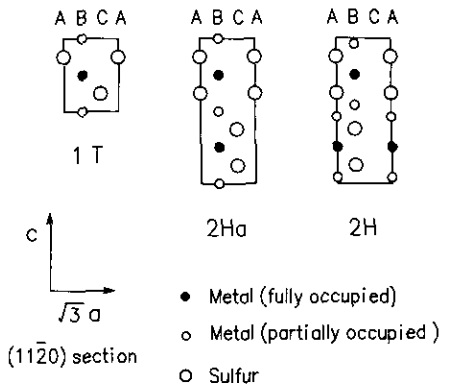

FIG. 1. Schematic figures for polytypes of MX_2 with (1120) section.

$2Ha$ polytype stacking sequence. On the other hand, the intercalated copper atoms are distributed over the tetrahedral holes between the prismatic TaS_2 layers and form the $2H$ polytype (see Fig. 1).

All the powder X-ray diffraction patterns of the compounds Mn_xTaS_2 in the range $0.20 \leq x \leq 0.50$ were indexed on the hexagonal unit cell of $2Ha$–TaS_2 (Fig. 1). Figure 2 shows the relationship between the manganese content x and the hexagonal lattice parameters a and c. It is clear from Fig. 2 that the lattice parameter c is almost constant beyond $x = 0.50$. And in the sample with manganese content x larger than 0.50, the reaction of deposited Mn with the silica ampule was observed. So the maximum content x of the single phase region was determined as $x = 0.50$. Mixed phases of $1T$-type and $2Ha$-type were observed in the powder X-ray diffraction patterns of the compounds Mn_xTaS_2 in the range $x < 0.20$. Accordingly it became clear that the single phase region is $0.20 \leq x \leq 0.50$ in Mn_xTaS_2 at 1000°C.

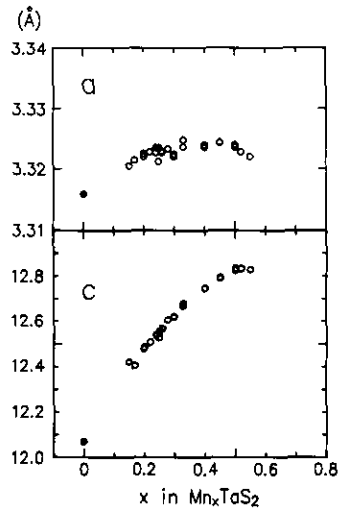

FIG. 2. Plots of hexagonal lattice parameters of Mn_xTaS_2.

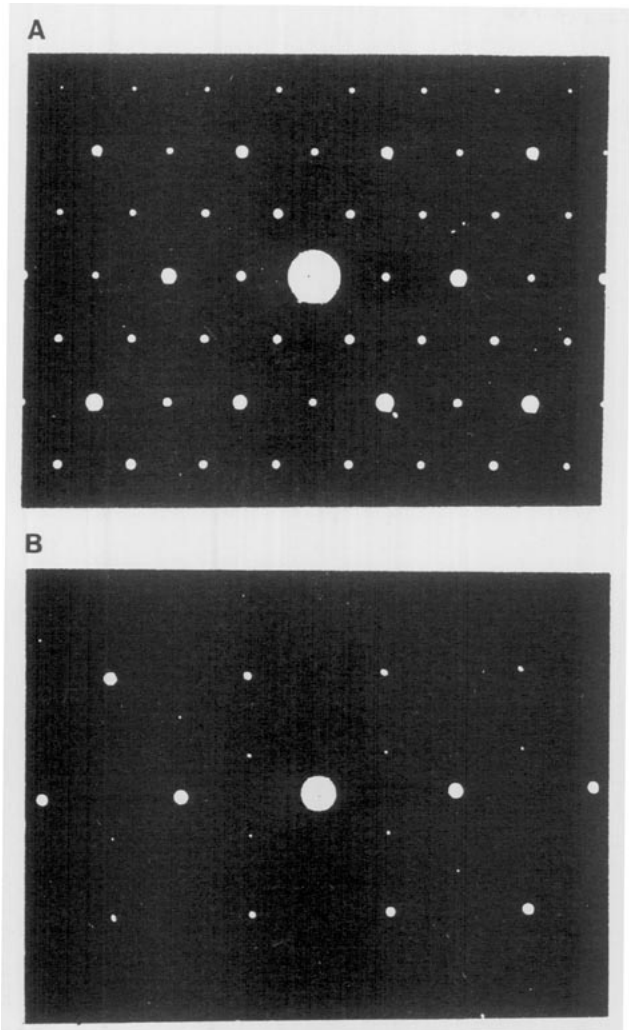

FIG. 3. Electron diffraction patterns for (A) $Mn_{1/4}TaS_2$ ($2a_0 \times 2a_0$ superlattice spots); and (B) $Mn_{1/3}TaS_2$ ($\sqrt{3}a_0 \times \sqrt{3}a_0$ superlattice spots).

In the single phase region, the lattice parameter c increased almost linearly with increasing manganese content x (Fig. 2), while the lattice parameter a had a broad maximum near $x = 1/3$. At the composition $x = 1/4$, an ordered $2a_0 \times 2a_0$ superlattice was found, where a_0 is the lattice parameter of the hexagonal basal plane of the host crystal (12). A $\sqrt{3}a_0 \times \sqrt{3}a_0$ superlattice is reported at $x = 1/3$ (4). The electron diffraction patterns for samples with $x = 1/4$ and $1/3$ from the present experiments are shown in Fig. 3. The superlattice spots which correspond to $2a_0 \times 2a_0$ and $\sqrt{3}a_0 \times \sqrt{3}a_0$ were also observed in the samples with compositions $x = 1/4$ and $1/3$, respectively. So the slight anomaly of the hexagonal lattice parameter a at $x = 1/4$ and $1/3$ in Fig. 2 would suggest the ordering of Mn atoms in the van der Waals gap plane at these compositions, and the behavior of the c parameter means that Mn ions inserted into the partially occupied layers expand the van der Waals gaps.

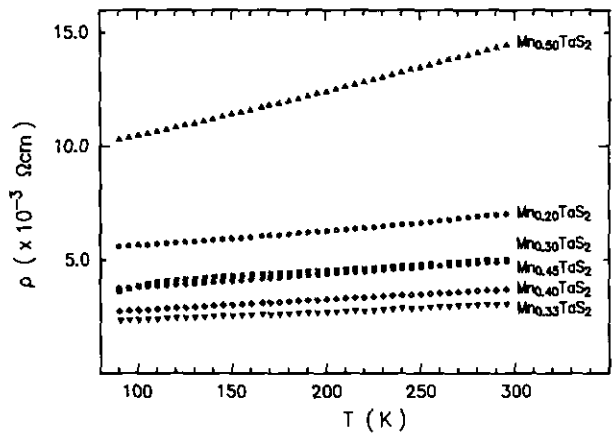

FIG. 4. Temperature variations of electrical resistivity of Mn_xTaS_2.

Figure 4 shows the electrical resistivity data in the temperature range from 90 to 300 K. In all the samples, the resistivity increased monotically with temperature, which indicates metallic behavior similar to that of $2Ha$–TaS_2 (9). Figure 5 shows the composition dependence of the electrical resistivity at room temperature. Resistivity measurements using single crystals have been obtained by Parkin and Friend; $\rho = 1.9 \times 10^{-4}$ ohm · cm for $Mn_{1/4}TaS_2$ and $\rho = 1.3 \times 10^{-4}$ hm · cm for $Mn_{1/3}TaS_2$ (9). The present data for $x = 1/4$ and $1/3$ were about one order of magnitude larger than the literature values; this would be due to the sintered powder samples. The electrical resistivity at room temperature decreased with increasing x had a minimum value at $x = 1/3$, and then increased with increasing x to a maximum value at $x = 1/2$, like Fe_xTaS_2 in our previous study (15). At the minimum composition the manganese atoms in the van der Waals gap were ordered in the $\sqrt{3}a_0 \times \sqrt{3}a_0$ superstructure, and this ordering seems to minimize the electrical resistivity.

Onuki *et al.* (14) estimated the charge transfer from the Mn atom to the mother crystal on $Mn_{1/4}TaS_2$ using the

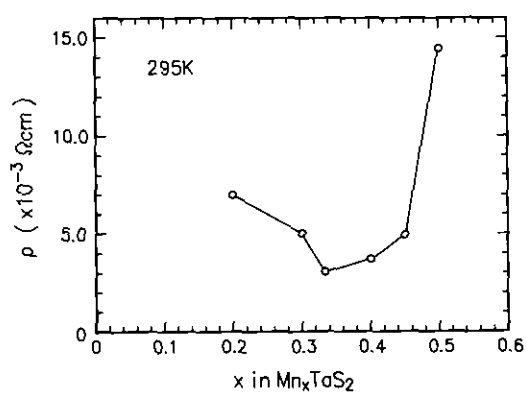

FIG. 5. Room temperature resistivity of Mn_xTaS_2.

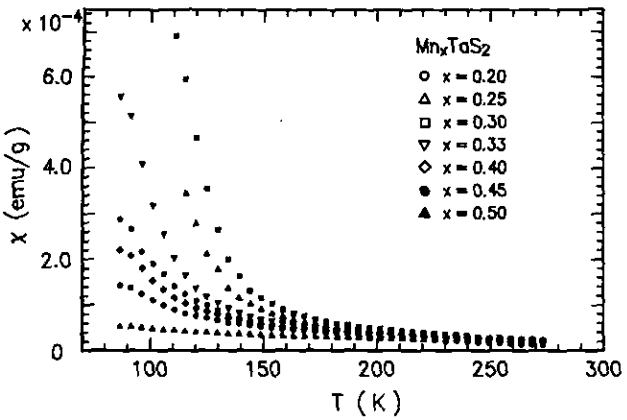

FIG. 6. Temperature dependence of magnetic susceptibilities of Mn_xTaS_2.

TABLE 1
Magnetic Parameters of Mn_xTaS_2

x in Mn_xTaS_2	θ (K)	P_{eff} (μ_B)
0.20	70.4	7.83
0.25	106.0	5.72
Ref. (14)	(113)	(5.30)
0.30	107.3	5.81
0.33	85.8	5.38
Ref. (18)	(83)	(4.67)
0.40	69.4	4.95
0.45	51.7	4.93
0.50	−21.9	4.90

measured Hall coefficients. They assumed that the Fermi level in TaS_2 lies in the middle of a d subband with a predominantly d_{z^2} character and that half of the band is empty, based on the rigid band model; they concluded that Mn is in a nearly divalent state at the composition $x = 1/4$. Parkin and Friend also concluded that the Mn ion is nearly divalent, and that this band model is applicable to $Mn_{1/3}TaS_2$ (9, 10). In our previous experiment (15), this rigid-band model could be applied to Fe_xTaS_2 ($0.20 \leq x \leq 0.50$). The resistivity in the present study at room temperature reached its largest value at $x = 0.50$, as shown in Fig. 5. Therefore, at $x = 0.50$, Mn atoms in the van der Waals gap donate one electron to the host molecular TaS_2 and the d_{z^2} subband is entirely filled, which suggests that the manganese ion is divalent, as was reported in the literature (7, 9–11).

Figure 6 shows the temperature dependence of magnetic susceptibilities. The susceptibility is fitted to a Curie–Weiss law of the form

$$\chi = \chi_0 + C_{mole}/(T - \theta),$$

where χ_0 is a temperature-independent term, θ is a Weiss constant, and C_{mol} is a molar Curie constant, from which an effective moment can be derived (16, 17). The relationship between temperature and inverse magnetic susceptibility is shown in Fig. 7. The values of C_{mol} and θ were obtained by using a least-squares refinement and are summarized in Table 1. The literature values for $x = 1/4$ and 1/3 are also listed in Table 1. The respective literature values of $\theta = 113$ K for $x = 1/4$ (12) and 83 K for $x = 1/3$ (18) agreed well with our present data. θ decreased with increasing manganese content x from $x = 0.25$ to 0.50 and was negative at $x = 0.50$, suggesting that the magnetic interactions changed from ferromagnetic to antiferromagnetic at $x = 0.50$ (see Fig. 8). This may originate from the shorter Mn–Mn distance in the van der Waals gap plane with the increase of manganese content x (19).

P_{eff} is an effective Bohr magneton per Mn atom calculated by using the values of C_{mol} (also listed in Table 1; see also Fig. 9). The effective Bohr magnetons of the spin-

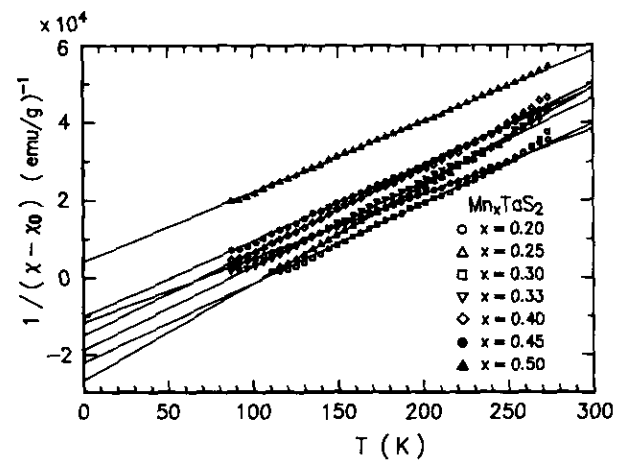

FIG. 7. Inverse magnetic susceptibility vs temperature of Mn_xTaS_2.

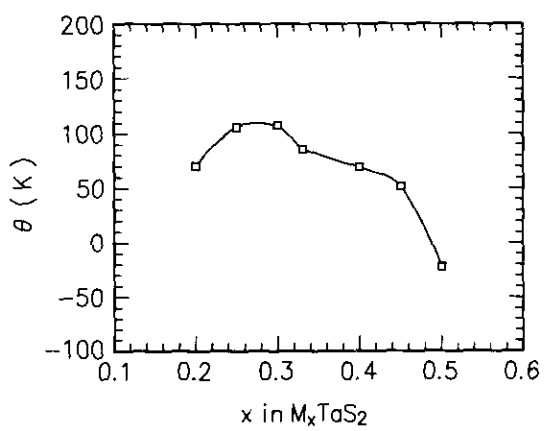

FIG. 8. Manganese content dependence of Weiss constants.

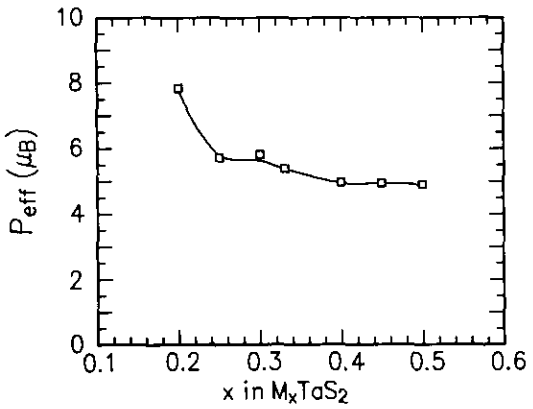

FIG. 9. Effective magnetic moment vs manganese content.

only values for Mn^{2+} and Mn^{3+} are 5.92 and 4.90 μ_B, respectively. The literature values for single crystals for $Mn_{1/4}TaS_2$ and $Mn_{1/3}TaS_2$ are 5.3 μ_B (12) and 4.67 μ_B (18), respectively. However, Parkin and Friend reported the μ_{eff} as $\perp c$ 6.08 μ_B and $\| c$ 5.97 μ_B for $Mn_{1/4}TaS_2$, and $\perp c$ 5.81 μ_B and $\| c$ 5.48 μ_B for $Mn_{1/3}TaS_2$ (7). The present results are 5.72 μ_B for $Mn_{1/4}TaS_2$ and 5.38 μ_B for $Mn_{1/3}TaS_2$. So the valence states of the Mn ions at x = 1/4 and 1/3 are both estimated to be divalent. The μ_{eff} value of the sample from x = 0.4 to 0.5 is around 5.0, and this value is very close to the spin-only Mn^{3+} value of 4.90 μ_B. However, Onuki *et al.* have reported (14) that

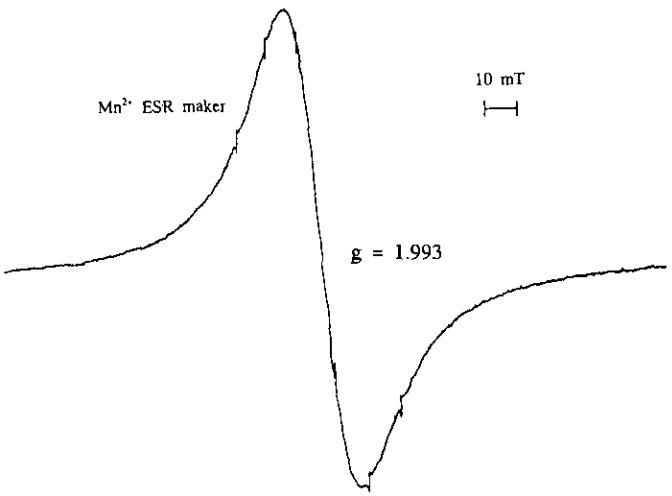

FIG. 10. The ESR signal for $Mn_{0.45}TaS_2$; the six spikes shown in the figure correspond to the Mn^{2+} ESR maker.

the exchange interaction between the Mn moments is mediated by the conduction electron through the RKKY interaction. Polarized neutron study (20) has confirmed that the moment on Mn sites depressed by ca. 15% compared with the expected value for the Mn^{2+} ion. In the present study, the signal corresponding to the Mn^{2+} ion was observed in all the samples by ESR measurements (shown in Fig. 10). Also, from the rigid-band estimate mentioned above, the Mn ion was suggested to be divalent at x = 0.50. Accordingly, we are able to conclude that the valence state of Mn ions in Mn_xTaS_2, $0.20 \leq x \leq 0.50$, is divalent.

ACKNOWLEDGMENT

We express our gratitude to Dr. Baba (Tokyo Institute of Technology) for performing the ESR measurements.

REFERENCES

1. J. A. Wilson, F. J. DiSalvo, and S. Mahajan, *Adv. Phys.* **24,** 117 (1975).
2. J. A. Woollam and R. B. Somoano, *Phys. Rev. B* **13,** 3843 (1976).
3. Y. Onuki, R. Inada, S. Tamura, S. Yamanaka, and H. Kamimura, *Synth. Met.* **5,** 245 (1983).
4. J. M. van den Berg and P. Cossee, *Inorg. Chim. Acta* **2,** 143 (1968).
5. K. Anzenhofer, J. M. van den Berg, P. Cossee, and J. N. Helle, *J. Phys. Chem. Solids* **31,** 1057 (1970).
6. T. Uchida, S. Satoh, M. Wakihara, and M. Taniguchi, *J. Chem. Soc. Jpn.* 1306 (1991).
7. S. S. P. Parkin and R. H. Friend, *Philos. Mag. B* **41,** 65 (1980).
8. W. B. Clark, *J. Phys. C* **9,** L693 (1976).
9. S. S. P. Parkin and R. H. Friend, *Philos. Mag. B* **41,** 95 (1980).
10. S. S. P. Parkin and A. R. Beal, *Philos. Mag., B* **42,** 627 (1980).
11. S. S. P. Parkin and S. C. Bayliss, *J. Phys. C* **15,** 6851 (1982).
12. B. van Laar, H. M. Rietvelt, and D. J. W. Ijdo, *J. Solid State Chem.* **3,** 154 (1971).
13. S. S. P. Parkin and E. A. Marseglia and P. J. Brown, *J. Phys. C* **16,** 2749 (1983).
14. Y. Onuki, K. Ina, T. Hirai, and T. Komatsubara, *J. Phys. Soc. Jpn.* **55,** 347 (1986).
15. H. Narita, H. Ikuta, H. Hinode, T. Uchida, T. Ohtani, and M. Wakihara, *J. Solid State Chem.* **108,** 148 (1994).
16. J. M. van den Berg, "Physics and Chemistry of Materials with Layered Structure: Optical and Electrical Properties" (P. A. Lee, Ed.). Reidel, Dordrecht, 1976.
17. A. R. Beal, "Physics and Chemistry of Materials with Layered Structure: Intercalated Layered Materials" (F. Levy, Ed.) Reidel, Dordrecht, 1979.
18. F. Hullinger and E. Pobitschka, *J. Solid State Chem.* **1,** 117 (1970).
19. P. F. Bongers, C. F. van Bruggen, J. Koopstra, W. P. F. A. M. Omloo, G. A. Wiegers, and F. Jellinek, *J. Phys. Chem. Solids* **29,** 977 (1968).
20. S. S. P. Parkin, E. A. Marseglia and P. J. Brown, *J. Phys. C* **16,** 2749 (1983).